Wind and Structures, *Vol. 27, No. 3 (2018) 175-186*
DOI: https://doi.org/10.12989/was.2018.27.3.175

Reliability analysis on flutter of the long-span Aizhai bridge

Shuqian Liu[1], C.S. Cai[1], Yan Han*[2] and Chunguang Li[2]

[1]*Department of Civil and Environmental Engineering, Louisiana State University, Baton Rouge, USA, LA 70803*
[2]*School of Civil Engineering, Changsha University of Science & Technology, Changsha, China, 410004*

(Received September 9, 2017, Revised January 28, 2018, Accepted February 24, 2018)

Abstract. With the continuous increase of span lengths, modern bridges are becoming much more flexible and more prone to flutter under wind excitations. A reasonable probabilistic flutter analysis of long-span bridges involving random and uncertain variables may have to be taken into consideration. This paper presents a method for estimating the reliability index and failure probability due to flutter, which considers the very important variables including the extreme wind velocity at bridge site, damping ratio, mathematical modeling, and flutter derivatives. The Aizhai Bridge in China is selected as an example to demonstrate the numerical procedure for the flutter reliability analysis. In the presented method, the joint probability density function of wind speed and wind direction at the deck level of the bridge is first established. Then, based on the fundamental theories of structural reliability, the reliability index and failure probability due to flutter of the Aizhai Bridge is investigated by applying the Monte Carlo method and the first order reliability method (FORM). The probabilistic flutter analysis can provide a guideline in the design of long-span bridges and the results show that the structural damping and flutter derivatives have significant effects on the flutter reliability, more accurate and reliable data of which is needed.

Keywords: flutter reliability; critical flutter velocity; long-span suspension bridges; flutter derivatives; Monte Carlo method; first order reliability method

1. Introduction

With the continuous increase of span lengths in recent years, modern bridges are becoming much more flexible and more prone to flutter under wind excitations, which has made flutter stability a major concern of long-span bridges design. In the past several decades, flutter stability of long-span bridges has been studied comprehensively and mature bridge flutter theories have been established (Agar 1998, Cai *et al*. 1999, Chen *et al*. 2000, Ge and Tanaka 2000, Ding *et al*. 2002, Hua and Chen 2008). Based on these theories, it is well acknowledged that bridge flutter occurs when the critical flutter velocity of the structure is exceeded by the extreme wind velocity at the bridge site. Typically, as long as the critical flutter velocity is higher than the extreme wind velocity at the bridge site, flutter stability is guaranteed. However, the critical flutter velocity and the extreme wind velocity are not deterministic but are affected by many uncertainties. The critical flutter velocity is usually obtained by either wind tunnel tests or numerical calculations with experimentally obtained flutter derivatives. Parameters used in both methods are typically treated as deterministic while many among them are actually uncertain variables, which may lead to unreliable results of the critical wind velocity. The basic wind velocity is usually based on design codes which can only provide a rough wind velocity of the bridge site, which is not adequate for a long-span bridge that may have a design life period of 100 years or longer. Therefore, it would be more reasonable to conduct a probabilistic flutter analysis of long-span bridges in which random and uncertain variables can be taken account of properly.

Compared to fruitful deterministic flutter analysis of bridges, the probabilistic flutter analysis is relatively rare. Ostenfeld-Rosenthal *et al*. (1992) performed the reliability analysis of flutter and proposed the probabilistic flutter criteria for long-span bridges, in which uncertainties considered were related to the prediction of extreme wind velocity, conversion from model to prototype, turbulence intensity, and structural damping. Ge *et al*. (2000) presented a reliability analysis model and three approaches to determine the probability of bridge failures due to flutter based on the first order reliability method (FORM). In this research, the basic flutter speed, which is considered as a log-normally distributed variable, is determined by an empirical formula. Pourzeynali and Datta (2002) conducted a reliability analysis of suspension bridges against flutter failure by considering various uncertainties such as geometric and mechanical properties of the bridge, modeling, damping, and flutter derivatives. Cheng *et al*. (2005) proposed a reliability analysis method in which the limit state function is constructed through the response surface method (RSM) and implicitly represented as a function of various variables. Baldomir *et al*. (2013) performed a reliability study for the proposed Messina Bridge by using FORM. In their study, each flutter derivative, as well as structural damping and extreme wind velocity, was considered as a random variable. According to the sensitivity analysis of various parameters by Cheng *et al*. (2005) and Pourzeynali and Datta (2002), the extreme wind velocity, damping ratio, modeling, and flutter derivatives are the most influential random variables on the

*Corresponding author, Professor
E-mail: ce_hanyan@163.com

http://www.techno-press.com/journals/was&subpage=7
ISSN: 1226-6116 (Print), 1598-6225 (Online)

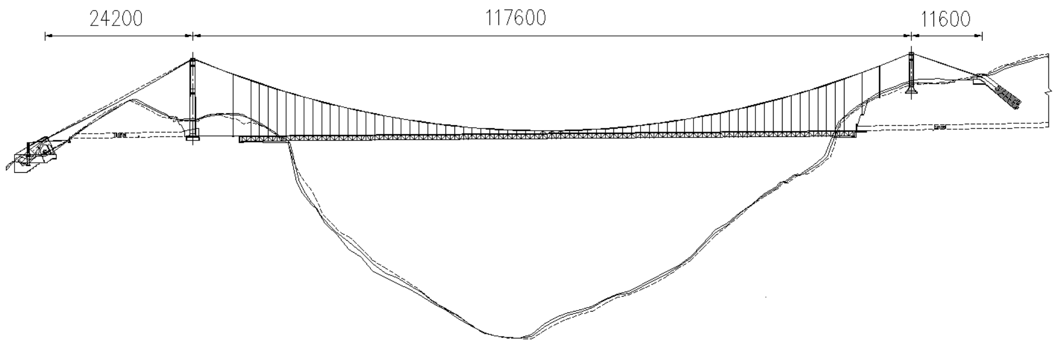

(a) Elevation view (unit: cm)

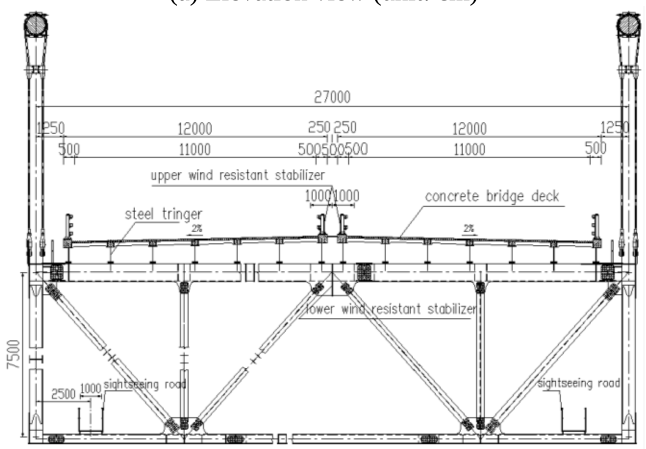

(b) Cross section (unit: mm)

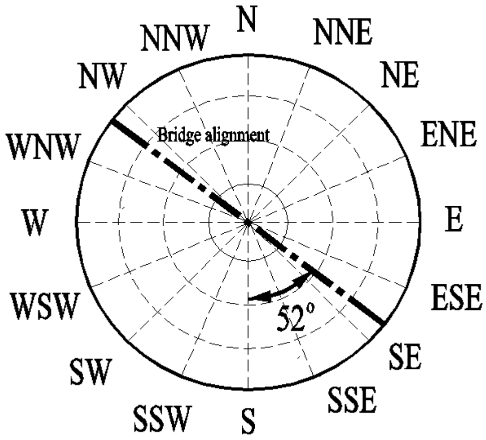

(c) Bridge alignment

Fig. 1 Aizhai Bridge

flutter reliability of long-span bridges, while the other random parameters such as material properties and geometric parameters have relative insignificant effects and can be regarded as constants in the flutter reliability analysis. When the other parameters such as stiffness and mass become more important in some special cases, one can consider these parameters following the established approach in the literature.

In the present paper, flutter reliability analysis is applied to a real bridge project with emphasis on several acknowledged important variables including the extreme wind velocity at the bridge site, damping ratio, mathematical modeling, and flutter derivatives. The extreme wind velocity at the bridge site, as the demand in the limit state function, is obtained by historical wind records of the nearby meteorological station and field measurements of anemometers installed on bridge, which can describe the wind distribution at the bridge site more accurately. The critical flutter velocity, as the resistance capacity in the limit state function, is determined by FEM in this study and affected by several uncertainties. Parametric studies of the uncertain variables to investigate their effects on the flutter reliability are conducted. Monte Carlo method and the first order reliability method (FORM) are applied here in the reliability analysis.

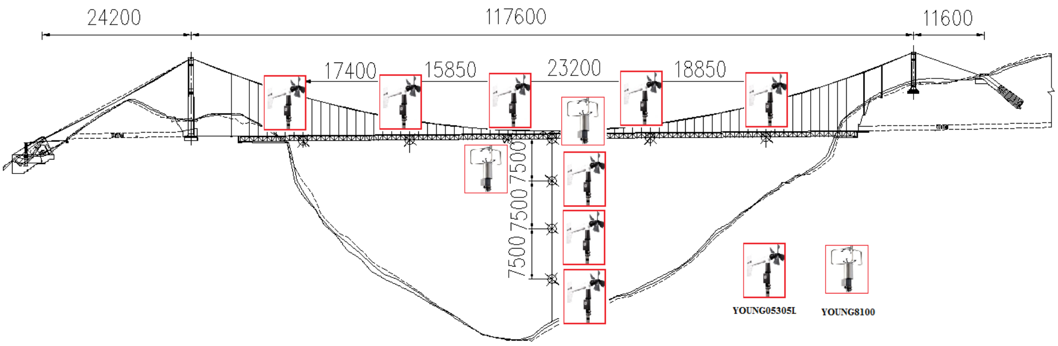

Fig. 2 Layout of anemometers on Aizhai Bridge (Unit: mm)

2. Aizhai Bridge

Aizhai Bridge is a single-span suspension bridge located in a mountainous area of China, with a main span of 1,176 m (steel truss girder) and two main cable side spans of 242 m and 116 m, as shown in Fig. 1(a). The width and height of the steel truss girder are 27 m and 7.5 m, respectively. The bridge deck is composite of steel stringers and a concrete slab. The rubber support is used between the steel girder and the upper beam of the main steel truss girder. The cross-section view of the bridge is displayed in Fig. 1(b). The bridge deck is suspended by suspenders in the main span. The bridge deck carries a dual two-lane highway on the deck. The alignment of the bridge deck deviates for 52^{o} in counterclockwise from the south axis, as shown in Fig. 1 (c).

A wind speed monitoring system was installed on the bridge to record the wind velocity at the bridge site, which has 10 anemometers in total. The monitoring system has been in operation for about two years currently. There were six anemometers (five YOUNG5305L and one YOUNG8100) along the longitudinal direction of the bridge, and four anemometers (three YOUNG5305L and one YOUNG8100) along the vertical direction of the bridge, as shown in Fig. 2.

3. Distribution of wind velocity and wind direction at the bridge site

Due to the difficulty and high cost of obtaining the wind velocity data at the bridge site for a consecutive long period, the distribution of wind velocity and wind direction is often estimated by utilizing the data of nearby meteorological stations. As is well known, the cumulative distribution of extreme wind values extracted from historical records tends to fit the asymptotic extreme-value distributions such as the extreme value type I (i.e., the Gumbel distribution), the extreme value type II (i.e., the Frechet distribution), and the extreme value type III (i.e., the Weibull distribution) (Mayne 1979; Palutikof *et al*. 1999). In this study, the distribution of wind velocity and direction at bridge site was obtained based on the nearby Jishou meteorological station and field measured wind speed data at the Aizhai Bridge site. First, the original data of the wind velocity and direction for a period of 31 consecutive years at the Jishou meteorological station was collected and the statistical analysis was conducted. Second, the probability distribution model of the wind velocity and direction was optimally determined among Gumbel, Frechet, and Weibull distributions. Last but not least, the distribution of the wind velocity and direction at the Aizhai Bridge site was determined according to the field measurements and the previously obtained probability distribution model.

3.1 Statistical analysis of wind data

The daily maximum values (10-min average) of the wind velocity at the height of 10m above the ground was obtained through sampling analysis. The results of the 16 compass directions and the non-directional sample (NDS) regardless of azimuth direction are shown in Table 1. The relative frequencies of wind direction are given in polar in Fig. 3.

3.2 Joint distribution model of wind velocity and direction

Three types of extreme-value distribution models are utilized here to fit the statistical frequency of the daily maximum wind velocity in Table 1. The cumulative distribution function (CDF) and the probability density function (PDF) of each distribution model can be expressed as:

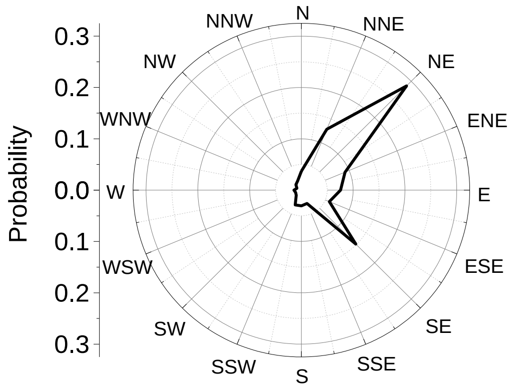

Fig. 3 Relative frequency of wind direction

Table 1 Frequency of daily maximum wind velocity at Jishou station

Comp. direct.	0-2 (m/s)	2-4 (m/s)	4-6 (m/s)	6-8 (m/s)	8-10 (m/s)	10-12 (m/s)	12-14 (m/s)	14-16 (m/s)	16-18 (m/s)	Frequency (%)
N	0.030	1.35	1.74	0.42	0.15	0	0	0.000	0.000	3.689
NNE	0.000	6.238	4.829	1.35	0.33	0.09	0	0.000	0.000	12.837
NE	0.000	10.018	14.037	3.75	0.75	0.15	0	0.000	0.000	28.704
ENE	0.000	2.22	4.649	1.86	0.33	0.06	0	0.000	0.000	9.118
E	0.000	2.73	3.54	1.02	0.24	0	0.03	0.000	0.000	7.558
ESE	0.030	2.88	2.52	0.36	0.03	0	0.03	0.000	0.000	5.849
SE	0.000	8.309	5.819	0.54	0.15	0.03	0	0.000	0.000	14.847
SSE	0.000	1.71	0.84	0.24	0.03	0	0	0.000	0.000	2.819
S	0.000	1.17	1.47	0.36	0	0.03	0.03	0.000	0.000	3.059
SSW	0.000	0.99	1.71	0.36	0.03	0.03	0	0.000	0.000	3.119
SW	0.000	0.6	0.72	0.06	0	0.03	0	0.000	0.000	1.410
WSW	0.000	0.48	0.42	0.3	0	0	0	0.000	0.000	1.200
W	0.000	0.45	0.6	0.27	0.09	0.03	0	0.000	0.000	1.440
WNW	0.000	0.12	0.3	0.36	0.09	0	0.06	0.000	0.000	0.930
NW	0.000	0.33	0.51	0.33	0.27	0.06	0	0.000	0.000	1.500
NNW	0.030	0.33	0.9	0.42	0.12	0.06	0.06	0.000	0.000	1.920
NDS	0.090	39.922	44.601	11.997	2.61	0.57	0.21	0.000	0.000	100.000

Gumbel distribution

CDF: $$P(u,\theta) = f(\theta).\exp\left[-\exp\left(-\frac{u-b(\theta)}{a(\theta)}\right)\right] \quad (1)$$

PDF: $$P(u,\theta) = f(\theta).\exp\left[-\exp\left(-\frac{u-b(\theta)}{a(\theta)}\right)\right].\exp\left(-\frac{u-b(\theta)}{a(\theta)}\right) \quad (2)$$

Frechet distribution

CDF: $$P(u,\theta) = f(\theta)\cdot\exp\left[-\left(\frac{u}{a(\theta)}\right)^{-\gamma(\theta)}\right] \quad (3)$$

PDF: $$P(u,\theta) = f(\theta)\cdot\frac{\gamma(\theta)}{a(\theta)}\cdot\exp\left[-\left(\frac{u}{a(\theta)}\right)^{-\gamma(\theta)}\right]\cdot\left(\frac{u}{a(\theta)}\right)^{-1-\gamma(\theta)} \quad (4)$$

Weibull distribution

CDF: $$P(u,\theta) = f(\theta)\cdot\left\{1-\exp\left[-\left(\frac{u}{a(\theta)}\right)^{\gamma(\theta)}\right]\right\} \quad (5)$$

PDF: $$P(u,\theta) = f(\theta)\cdot\frac{\gamma(\theta)}{a(\theta)}\cdot\exp[-(\frac{u}{a(\theta)})^{\gamma(\theta)}]\cdot(\frac{u}{a(\theta)})^{\gamma(\theta)-1} \quad (6)$$

in which $f(\theta)$ is the frequency of the compass direction θ; $a(\theta)$, $b(\theta)$, and $\gamma(\theta)$ are the scale parameter, location parameter, and shape parameter, respectively, in the distribution functions which can be optimally estimated according to the sample of wind velocity records of the corresponding wind direction.

It is assumed that the wind velocities of different directions follow the same distribution model, and the parameters in the distribution model of different wind directions are mutually independent (Ge and Xiang 2002). The least squares method was utilized to fit the parameters in each distribution model and the results are shown in Table 2. The probability density curves of the non-directional sample are shown in Fig. 4. According to Table 2, the correlation coefficients r of the Gumbel distribution are the largest among three distribution models. From Fig. 4, it can also be found that the best-fitted curve is the Gumbel distribution. Hence, it can be concluded that the maximum wind velocity follows the Gumbel distribution.

3.3 Distribution of wind velocity at the Aizhai Bridge site

As the Aizhai Bridge is close to the Jishou meteorological station, it is assumed that the wind direction distribution at the bridge site is the same as the meteorological station. The joint distribution function of the wind velocity and direction at the meteorological station is expressed as

Table 2 Wind distribution parameters

Comp. direct.	$f(\theta)$	Gumbel distribution			Frechet distribution			Weibull distribution		
		a	b	r	A	Γ	r	a	γ	r
N	0.037	1.27	3.990	0.975	4.048	2.983	0.940	4.78	3.635	0.953
NNE	0.128	1.294	3.523	0.982	3.605	2.742	0.972	4.462	3.061	0.938
NE	0.287	1.2	4.065	0.998	4.161	3.260	0.959	4.825	3.780	0.968
ENE	0.091	1.232	4.410	0.990	4.523	3.783	0.985	5.219	3.796	0.928
E	0.076	1.047	4.000	0.981	4.088	3.789	0.979	4.748	3.926	0.902
ESE	0.058	0.891	3.688	0.992	3.69	3.980	0.988	4.29	4.251	0.912
SE	0.148	0.895	3.537	0.994	3.519	3.884	0.971	4.097	4.430	0.979
SSE	0.028	0.754	3.370	0.933	3.35	4.577	0.962	3.742	5.296	0.839
S	0.031	1.128	3.849	0.961	3.869	3.173	0.900	4.502	4.068	0.970
SSW	0.031	1.191	4.202	0.972	4.407	4.159	0.925	4.927	4.037	0.992
SW	0.014	1.006	3.881	0.976	3.921	3.744	0.956	4.616	4.048	0.931
WSW	0.012	1.602	3.921	0.829	3.968	2.336	0.783	5.145	2.800	0.816
W	0.014	1.757	4.386	0.921	4.449	2.249	0.811	5.573	3.013	0.943
WNW	0.009	1.992	5.510	0.568	5.667	3.132	0.542	6.863	3.397	0.630
NW	0.015	2.015	4.980	0.728	5.005	2.409	0.763	6.632	2.639	0.658
NNW	0.019	1.236	4.614	0.905	4.658	3.869	0.910	5.549	3.855	0.838
NDS	1.000	1.187	4.391	1.000	4.433	3.572	0.978	5.139	4.041	0.955

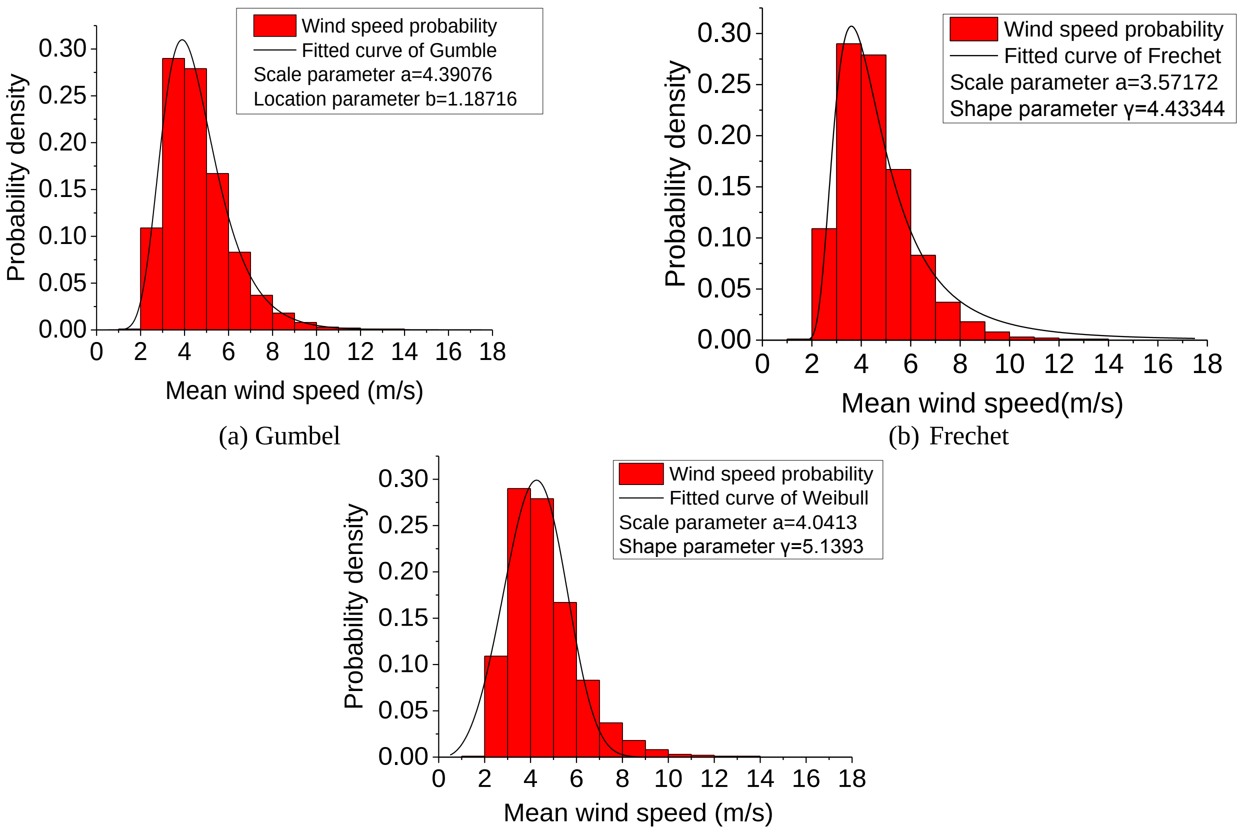

(a) Gumbel

(b) Frechet

(c) Weibull

Fig. 4 Probability density curve of NDS

Table 3 Wind distribution parameters at bridge site

Comp. direct.	a_{bi}	b_{bi}	μ_{ub}	σ_{ub}	U_{100}	p_i
N	2.197	6.903	8.171	2.818	17.019	0.037
NNE	2.239	6.095	7.387	2.871	16.402	0.128
NE	2.076	7.032	8.231	2.662	16.591	0.287
ENE	2.131	7.629	8.860	2.733	17.443	0.091
E	1.811	6.920	7.965	2.323	15.260	0.076
ESE	1.541	6.380	7.270	1.977	13.477	0.058
SE	1.548	6.119	7.013	1.986	13.248	0.148
SSE	1.304	5.830	6.583	1.673	11.836	0.028
S	1.951	6.659	7.785	2.503	15.644	0.031
SSW	2.060	7.269	8.459	2.643	16.756	0.031
SW	1.740	6.714	7.719	2.232	14.727	0.014
WSW	2.771	6.783	8.383	3.554	19.544	0.012
W	3.040	7.588	9.342	3.898	21.583	0.014
WNW	3.446	9.532	11.521	4.420	25.399	0.009
NW	3.486	8.615	10.627	4.471	24.666	0.015
NNW	2.138	7.982	9.216	2.742	17.827	0.019
NDS	2.054	7.596	8.782	2.634	17.051	1

Note: NDS= non-directional sample

$$P(u_0,\theta)=f(\theta).g(u_0) \tag{7}$$

where $f(\theta)$ is the frequency of the compass direction θ, which is assumed the same for both the meteorological station and the bridge site; $g(u_0)$ denotes the cumulative distribution function of the corresponding wind velocity.

Assume that the gradient wind velocities at the meteorological station and the bridge site are equal, the relationship between the wind velocities at the meteorological station and different heights at the bridge site can be established as follows

$$\frac{U_b}{U_0}=\left(\frac{H_0}{h_0}\right)^{\alpha_0}\cdot\left(\frac{h_b}{H_b}\right)^{\alpha_b} \tag{8}$$

in which H_0 and H_b are the gradient wind heights at the meteorological station and the bridge site, respectively; h_0 and h_b are the height of observation point where the ground is flat and relatively wide at the meteorological station and the height of the bridge deck; α_0 and α_b are surface roughness exponents at the meteorological station and the bridge site, respectively.

At the meteorological station, the height of observation point h_0 is 10 m, the surface roughness exponent is set as 0.16 and the gradient wind height H_0 is set as 350 m according to Terrain type B due to the relatively flat and wide ground. At the bridge site, the surface roughness exponent α_b can be determined using field measurements. As is mentioned before, there are 10 anemometers in total installed on the Aizhai Bridge, which can provide real-time wind velocities at the bridge site. The wind profile at the bridge site was simulated according to the field measured wind velocities of the four vertical anemometers, as shown in Fig. 5 with four data sets (data 1 to data 4), where Z_1 and Z_2 are the heights of the reference point and the monitoring point, respectively, and U_{Z1} and U_{Z2} are the wind velocities of the corresponding heights. It can be found that the surface roughness exponent α_b is 0.215, which indicates that the wind field at the bridge site belongs to Terrain type C. Thus, the gradient wind height H_b is set as 400 m. The height of the bridge deck h_b cannot be taken as the height from the ground to the deck for the mountain valley terrain. In this paper, the height of the bridge deck h_b is defined as the equivalent height equal to the area enclosed by the ground surface and the girder divided by the girder length according to the area equivalence criterion.

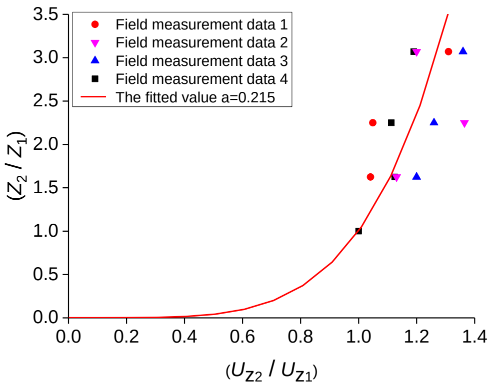

Fig. 5 Wind profile at the bridge site

Based on Eqs. (7) and (8) and the previously obtained Gumbel distribution parameters at the meteorological station, the distribution of wind velocity at the Aizhai Bridge site can be determined.

The Gumbel distribution parameters a_{bi} and b_{bi}, the mean μ_{ub} and the standard derivative σ_{ub}, the maximum wind velocity over 100-year return period U_{100}, and the relative frequency of occurrence p_i of the 16 wind directions and the non-directional sample (NDS) regardless of azimuth direction are calculated and shown in Table 3.

4. Distribution of critical flutter velocity of bridge

In this study, the critical flutter velocity is based on the result of numerical calculation by FEM, taking account of the uncertainties including damping ratio, mathematical modeling, and experimentally obtained flutter derivatives. The critical flutter velocity here is represented by a basic flutter velocity multiplied by three factors of uncertainties, which can be expressed as follows

$$U_{cr} = U_f F_d F_m F_{fd} \tag{9}$$

in which U_{cr} is the critical flutter velocity, U_f is the basic flutter velocity determined by FEM which contains several uncertainties. F_d, F_m and F_{fd} denote the effects of the structural damping uncertainty, the modeling uncertainty, and the flutter derivatives uncertainty on the basic flutter velocity U_f, respectively. All these uncertainty factors are assumed as independent log-normal distributed random variables with mean value of unity (Pourzeynali and Datta 2002).

4.1 Basic flutter velocity by FEM

The equation of motion of a bridge in the smooth flow can be expressed as

$$\mathbf{M}\ddot{\mathbf{q}} + \mathbf{C}\dot{\mathbf{q}} + \mathbf{K}\mathbf{q} = \mathbf{F}_{se} \tag{10}$$

where $\mathbf{M}$, $\mathbf{C}$, and $\mathbf{K}$ are the global mass, damping, and stiffness matrices, respectively; $\mathbf{q}$, $\dot{\mathbf{q}}$, and $\ddot{\mathbf{q}}$ represent the nodal displacement, velocity, and acceleration vectors, respectively; and $\mathbf{F}_{se}$ denotes the vector of the nodal aeroelastic forces.

Self-excited lift force L_{se}, drag force D_{se}, and pitching moment M_{se} per unit length of bridge deck are defined as (Scanlan 1978)

$$L_{se} = \frac{1}{2}\rho U^2 B[KH_1^*\frac{\dot{h}}{U} + KH_2^*\frac{B\dot{\alpha}}{U} + K^2H_3^*\alpha + K^2H_4^*\frac{h}{B} + KH_5^*\frac{\dot{p}}{U} + K^2H_6^*\frac{p}{B}] \tag{11a}$$

$$D_{se} = \frac{1}{2}\rho U^2 B[KP_1^*\frac{\dot{p}}{U} + KP_2^*\frac{B\dot{\alpha}}{U} + K^2P_3^*\alpha + K^2P_4^*\frac{p}{B} + KP_5^*\frac{\dot{h}}{U} + K^2P_6^*\frac{h}{B}] \tag{11b}$$

$$M_{se} = \frac{1}{2}\rho U^2 B^2[KA_1^*\frac{\dot{h}}{U} + KA_2^*\frac{B\dot{\alpha}}{U} + K^2A_3^*\alpha + K^2A_4^*\frac{h}{B} + KA_5^*\frac{\dot{p}}{U} + K^2A_6^*\frac{p}{B}] \tag{11c}$$

in which ρ is the air density; U is the mean wind velocity; B is the bridge deck width; K is the reduced circular frequency; H_i^*, P_i^* and A_i^* (i =1 to 6) are the aerodynamic derivatives related to the vertical, lateral, and torsional directions, respectively; h, p, and α are the vertical, lateral, and torsional displacements of the bridge, respectively; and
the dot on the cap denotes the derivative with respect to the time.

A three-dimensional finite element model of the Aizhai Bridge has been established to calculate the basic critical flutter velocity, as shown in Fig. 6. The bridge deck is modeled by beam188 elements. The main cables and suspension cables are simulated by link10 elements. The structural damping ratio is assumed as 0.5%. According to the flutter derivatives experimentally determined by wind tunnel forced vibration tests, 3D flutter analysis of the Aizhai Bridge has been carried out by FEM in ANSYS (Hua *et al*. 2007, Han *et al*. 2015).

In finite element analysis, the aerodynamic forces in Eq. (11) are incorporated in Eq. (10) in terms of aerodynamic stiffness and damping matrices, which are expressed by parameters such as flutter derivatives, wind velocity, and reduced circular frequency. A pair of Matrix27 elements are attached to each node of the bridge deck to model the aerodynamic force matrices, one for the stiffness matrix and one for the damping matrix. Thus, the governing equation of motion for the bridge can be derived as

$$\mathbf{M}\ddot{\mathbf{q}} + (\mathbf{C} - \mathbf{C}_{ae})\dot{\mathbf{q}} + (\mathbf{K} - \mathbf{K}_{ae})\mathbf{q} = \mathbf{0} \tag{12}$$

where $\mathbf{C}_{ae}$ and $\mathbf{K}_{ae}$ denote the aerodynamic damping and stiffness matrices, respectively.

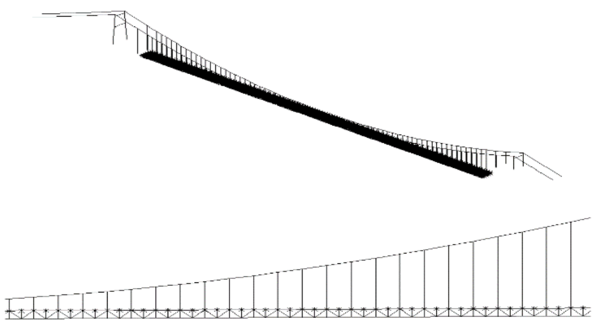

Fig. 6 Finite element model of Aizhai Bridge

Table 4 Critical flutter velocity of Aizhai Bridge

Method	Critical flutter velocity (m/s)
Section model test	77.1
FEM	78

By solving Eq. (12), the critical flutter velocity can be determined through the damped complex eigenvalue analysis. If the real part of one eigenvalue becomes zero at a certain wind velocity, then the system is on the critical flutter state and the corresponding wind velocity is the critical flutter wind velocity. The result of the critical flutter velocity at the wind attack angle of 0° by FEM, compared with the result of the section model wind tunnel test, is shown in Table 4. It can be found that the results of these two methods are consistent (within numerical errors), which indicates the accuracy of the critical flutter velocity by FEM.

4.2 Damping ratio uncertainty

For long-span suspension bridges, which are very flexible and vulnerable to wind effects, structural damping is one of the most important parameters for aerodynamic safety of the structure. However, there are relatively very rare data of measurements of structural damping for long-span suspension bridges. According to Davenport and Larose (1989), the structural damping of long-span bridges can be described as

$$\zeta = \frac{c}{f} E \tag{13}$$

in which ζ is the damping ratio to critical damping ratio (%); c is the proportionality coefficient; f is the structural frequency (Hz); E is a log-normally distributed uncertainty factor with mean value of unity and coefficient of variation equal to 0.4.

As is mentioned before, the structural damping ratio is equal to 0.5% ($\mu_\zeta = \frac{c}{f} = 0.5$). Hence, the standard deviation of ζ can be derived as

$$\sigma_\zeta = \frac{c}{f} COV(E) = 0.2 \tag{14}$$

According to a study by Ostenfeld-Rosenthal *et al.* (1992) based upon the thin airfoil theory, a linear function between the critical flutter velocity and the structural damping is assumed and the linear fitting result is as follows

$$U_{cr} = 76.9 + 2.2\zeta \tag{15}$$

Hence, the standard deviation of the structural damping uncertainty factor F_d can be derived as

$$\sigma_{F_d} = 2.2\sigma_\zeta = 0.44 \tag{16}$$

4.3 Mathematical modeling uncertainty

As is stated before, the basic flutter velocity is determined by FEM in ANSYS. However, the finite element model is an idealized model, which may not fully represent the actual structure due to several assumptions, approximations, and simplifications in the modeling. There may also have some errors in the numerical calculation. All these uncertainties that may affect the basic flutter velocity are considered here by introducing a modeling uncertainty factor F_m. Referring to the research by Pourzeynali and Datta (2002), the standard deviation of the modeling uncertainty factor F_m is assumed as 0.1.

4.4 Flutter derivatives uncertainty

As is mentioned before, the experimentally obtained flutter derivatives are essential for the numerical calculation of the basic flutter velocity. For the application of example in this paper, the flutter derivatives are determined in the HD-2 wind tunnel of Hunan University. According to Pourzeynali and Datta (2002), the uncertainty of flutter derivatives may arise from the turbulence effect, the experimental error, and curve-fitting techniques. It is found by Scanlan (1997) that the turbulence effects can increase the critical flutter velocity by 10% to 20% over that under smooth flow. Bucher and Lin (1988) also proved that the presence of turbulence may be favorable for flutter stability of bridges if there exists of aerodynamic coupling between the structural modes of vibration. Therefore, it will be more conservative to retain smooth-flow flutter derivatives for design studies. As a consequence, the turbulence effect on flutter derivatives is ignored here.

According to a comparative and sensitivity study of flutter derivatives by Sarkar *et al*. (2009), the differences in flutter derivatives are mainly attributed to different experimental methods (free or forced vibration) used in wind tunnel tests, different laboratory environments or operational conditions, and effects of amplitude dependency of the aero-elastic terms (for bluff cross sections). The flutter derivatives of the Aizhai Bridge by free vibration tests and forced vibration tests, compared with Theodorsen function, are shown in Fig. 7. It can be found that there are relatively large irregular fluctuations in the values of the free vibration test, especially for H_4^* and A_4^*. For A_2^* and A_3^*, the values of the free vibration and forced vibration tests are relatively consistent at the low reduced wind velocities. Compared with the free vibration test, the identification accuracy of the forced vibration test is relatively higher and the range of the reduced wind velocity is larger. As a result, the flutter derivatives used in this study are obtained by forced vibration test. According to Sarkar *et al*. (2007), due to the flutter derivative uncertainty, flutter velocity uncertainty value varies from 5% to 30%. Because of the lack of sufficient knowledge of flutter derivative distributions and their effects on flutter velocity, the standard deviation of the flutter derivatives uncertainty factor F_{fd} is assumed as 0.15 in the following flutter reliability analysis.

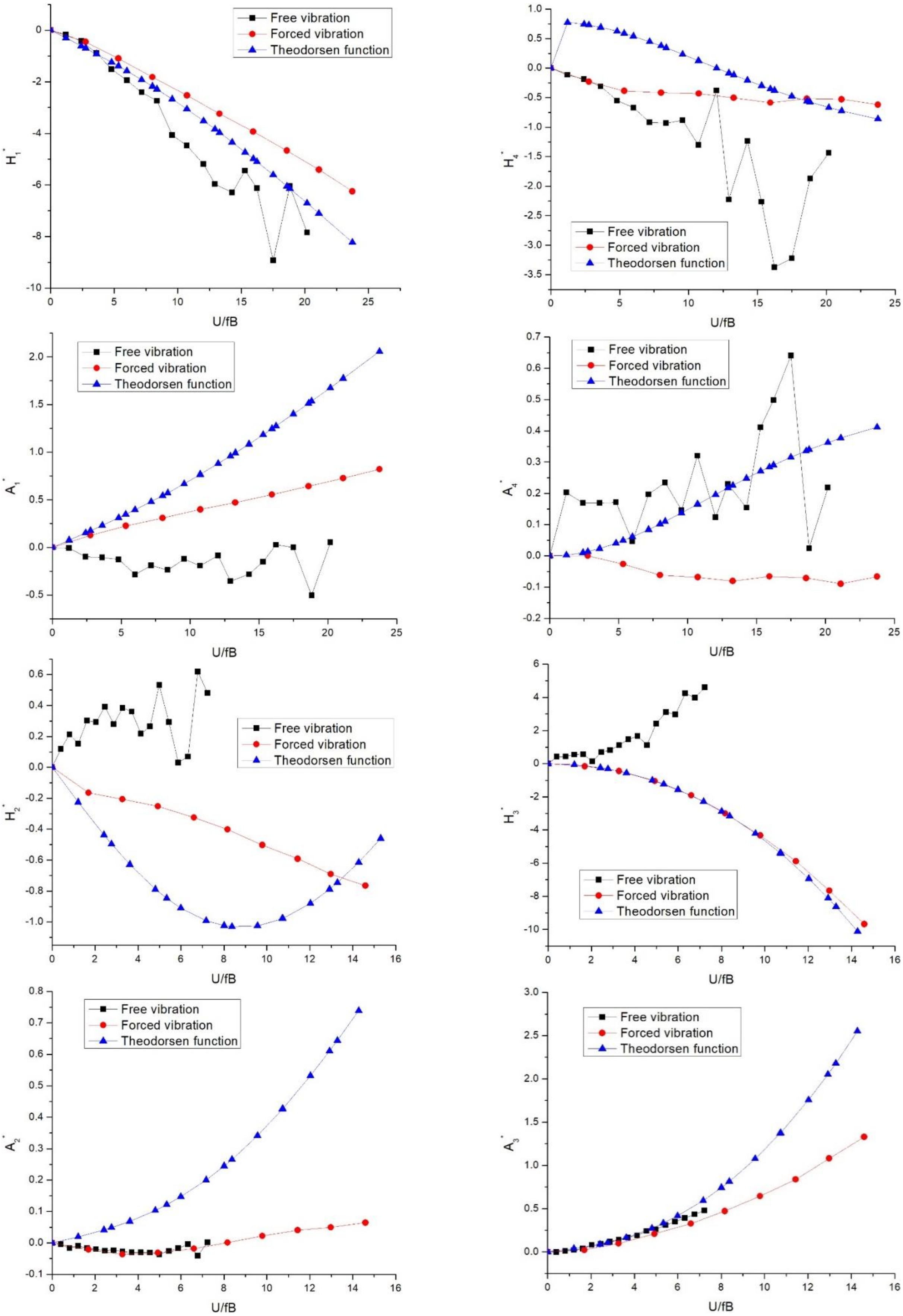

Fig. 7 Flutter derivatives of Aizhai Bridge

Table 5 Parameters of the random variables

Random variable	Distribution type	Mean value			Standard deviation		
		Case Ⅰ	Case Ⅱ	Case Ⅲ	Case Ⅰ	Case Ⅱ	Case Ⅲ
U_e	Gumbel	N/A	8.231	8.782	N/A	2.662	2.634
F_d	Lognormal		1			0.44	
F_m	Lognormal		1			0.1	
F_{fd}	Lognormal		1			0.15	

Table 6 Results of flutter reliability analysis

Case	Monte Carlo method		AFORM	
	β	P_f	β	P_f
Ⅰ	4.0419	2.6509e-05	4.0315	2.7713e-05
Ⅱ	3.9215	4.4000e-05	3.9211	4.4074e-05
Ⅲ	3.8643	5.5700e-05	3.8711	5.4179e-05

5. Flutter reliability analysis

The limit state function for flutter reliability analysis is defined as follows

$$f(F_d, F_m, F_{fd}, U_e) = U_f F_d F_m F_{fd} - U_e \qquad (17)$$

in which U_f is the basic flutter velocity of bridge, U_e is the extreme wind velocity at the bridge site. F_d, F_m and F_{fd} are the structural damping uncertainty factor, the modeling uncertainty factor, and the flutter derivatives uncertainty factor, respectively.

As is well known, bridge flutter is mainly caused by cross winds. Hence, only the wind component in the direction perpendicular to the longitudinal axis of the bridge is considered in the flutter reliability analysis. For each particular compass direction, the extreme wind velocity is

$$U_e = U_i \cos\theta_i \qquad (i = 1, 2, \ldots, 16) \qquad (18)$$

where U_i is the wind velocity in the compass direction *i*, θ_i is the yaw angle between the compass direction *i* and the direction perpendicular to the longitudinal axis of the bridge.

According to the relative frequencies of occurrence of all 16 compass directions in Table 3, the probability of failure due to flutter can be derived as

$$P_F = \sum_{i=1}^{16} p_i P_{F_i} \qquad (19)$$

in which p_i is the relative frequency of occurrence of compass direction *i*, P_{F_i} is the probability of failure of compass direction *i* with the extreme wind velocity of $U_i \cos\theta_i$.

The methodology mentioned above has taken account of the relative occurrence frequencies of wind directions, which will be more reasonable and precise. For comparison, the NE direction, which is almost perpendicular to the longitudinal axis of the bridge as shown in Fig. 3, and the non-directional sample (NDS) have also been studied by ignoring the frequency of occurrence. The three cases, namely, the one considering all 16 compass directions and their relative occurrence frequencies, the NE direction only, and the NDS respectively, are defined as case I, case II, and case III below, respectively.

The distribution parameters of random variables in the limit state function, which are obtained previously, are summarized in Table 5. All these random variables are assumed mutually independent. Based on the well-developed structural reliability theories, Monte Carlo method, and the advanced first order reliability method (AFORM) are adopted here to conduct the flutter reliability analysis of the Aizhai Bridge for mutual verifications. The results of the reliability index β and probability of failure P_f are shown in Table 6. It can be found that the reliability index of the NE direction (case II) without considering the occurrence frequency of this direction is close to that of case I which considers the occurrence frequencies of all 16 compass directions. The results of case III are the most conservative among three cases. Though the result of case I is most precise one, the result of the NE direction (case II) can still be utilized as reference for the preliminary design for simplification and is more conservative, especially for circumstances that lack of enough wind data of other wind directions

6. Parametric analysis of uncertainty factors

As is stated before, three uncertainty factors are introduced to estimate the effects of the structural damping uncertainty, the modeling uncertainty, and the flutter derivatives uncertainty on the basic flutter velocity, respectively. Parametric studies of three factors are conducted separately to investigate the sensitivity of these parameters on the flutter reliability index. The estimation of the structural damping is one of the most difficult problems in structural dynamics. Based on the database of Davenport and Carroll (1986), the coefficient of variation (COV) of the structural damping of high-rise buildings can range from 33% to 78%. Due to the lack of sufficient data of long-span bridges, the range of the COV of the structural damping uncertainty factor F_d is set as from 0.3 to 0.8 with intervals of 0.1 here. As the results of the critical wind velocity by FEM and by the section model wind tunnel test are highly consistent, the accuracy of the finite element model is warranted. Hence, the COV of the modeling uncertainty factor F_m is assumed to vary from 5% to 15% with uniform increments of 5%. The flutter derivatives uncertainty factor is one of the most influential variables on the reliability of long-span suspension bridges. It was also found by Sarkar *et al*. (2007) that the flutter derivative uncertainty did not directly relate to flutter velocity uncertainty.

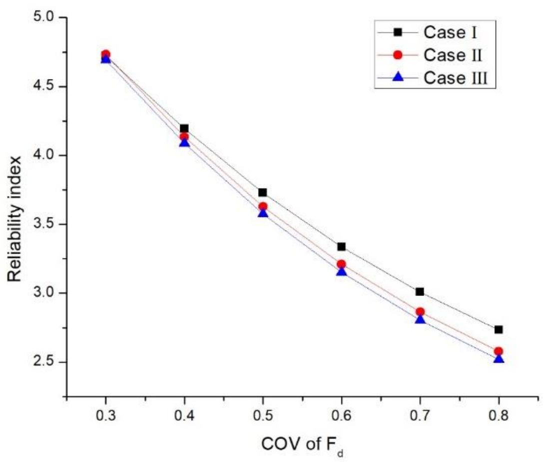

Fig. 8 Values of reliability index versus COV of F_d

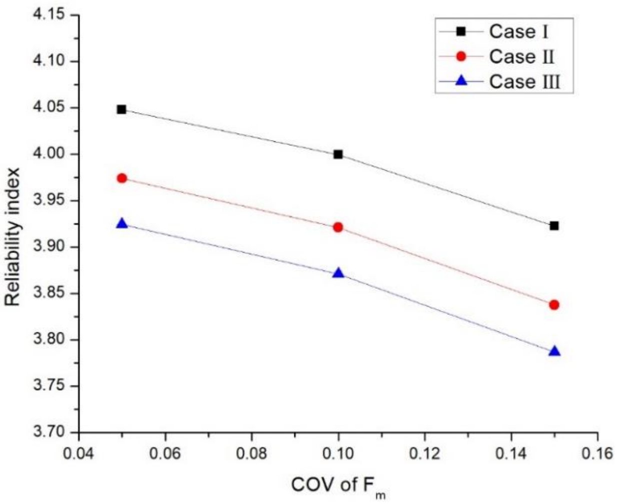

Fig. 9 Values of reliability index versus COV of F_m

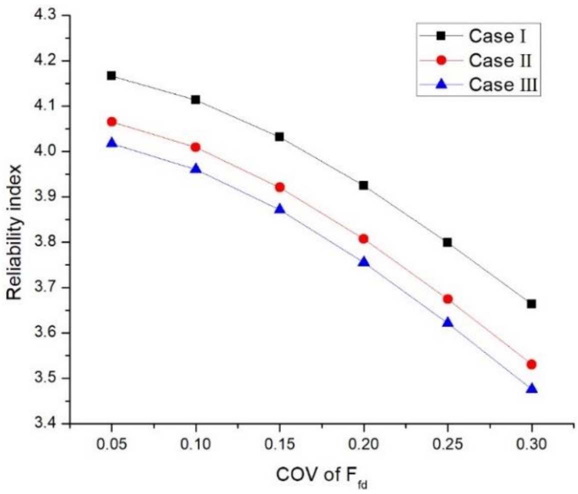

Fig. 10 Values of reliability index versus COV of F_{fd}

This is understandable because the flutter velocity depends heavily on the type of bridge and mode of flutter. Flutter velocity uncertainty values that are partly resulted from the flutter derivative uncertainties, can range from 5% to 30% depending on various conditions. As a result, the COV of the flutter derivatives uncertainty factor F_{fd} is assumed ranging from 0.05 to 0.3 with intervals of 0.05. The results of parametric studies are shown in Figs. 8-10. It can be found that the reliability index decreases with the increase of the coefficient of variation for all three factors. Compared with the modelling uncertainty, the structural damping and the flutter derivatives have more significant effects on the flutter reliability of bridges, especially for the structural damping, which causes a maximum variation of the reliability index as large as 46.4%.

7. Conclusions

A reliability analysis model is established and an application is conducted to investigate the reliability of long-span bridges against flutter failure. Uncertainties considered in the reliability analysis are the extreme wind velocity at the bridge site, damping ratio of bridge, and flutter derivatives. The extreme wind velocity at the bridge site is proven to follow the Gumbel distribution. The uncertainty of modeling has relatively small impact on the reliability index. It is found that the uncertainties of structural damping and flutter derivatives have significant effects on the flutter reliability of long-span suspension bridge, which indicates that it is important and necessary to obtain more accurate and reliable information of these parameters. The reliability index can provide more reasonable guidance than the critical flutter velocity for long-span bridges design. The reliability analysis method proposed here can be applied to obtain more adequate understanding of the flutter stability performance of long-span bridges.

Acknowledgements

This work described in this paper is supported by the key basic research project (973 project) of P.R. China, under contract No. 2015CB057701 and 2015CB057706 and by Hunan Provincial Education Department scientific research outstanding youth project under contract No. 16B011. And the authors would also like to gratefully acknowledge the supports from the National Science Foundation of China (No. 51678079; 51628802) and the School of Civil Engineering and Architecture, Changsha University of Science and Technology.

References

Agar, T.J.A. (1998), "The analysis of aerodynamic flutter of suspension bridges", *Comput. Struct.*, **30**(3), 593-600.

Baldomir, A., Kusano, I., Hernandez, S. and Jurado, J.A. (2013), "A reliability study for the Messina Bridge with respect to flutter phenomena considering uncertainties in experimental and numerical data", *Comput. Struct.*, **128**, 91-100.

Bucher, C.G., and Lin, Y.K. (1988), "Stochastic stability of bridges considering coupled modes", *J. Eng. Mech.*, **114**(12), 2055-2071.

Cai, C. S., Albrecht, P. and Bosch, H.R. (1999), "Flutter and buffeting analysis. II: Luling and Deer Isle bridges", *J. Bridge Eng.*, **4**(3), 181-188.

Chen, X., Matsumoto, M. and Kareem, A. (2000), "Time domain flutter and buffeting response analysis of bridges", *J. Eng. Mech.*, **126**(1), 7-16.

Cheng, J., Cai, C.S., Xiao, R.C. and Chen, S.R. (2005), "Flutter reliability analysis of suspension bridges", *J. Wind Eng. Ind. Aerod.*, **93**(10), 757-775.

Davenport, A.G. and Larose, G.L. (1989), "The structural damping of long span bridges, an interpretation of observations", *Proceedings of the Canada-Japan Workshop on Bridge Aerodynamics.*

Davenport, A.G. and Hill-Carroll, P. (1986), "Damping in tall buildings: its variability and treatment in design", *Build. Motion Wind ASCE*, 42-57.

Ding, Q., Chen, A. and Xiang, H. (2002), "Coupled flutter analysis of long-span bridges by multimode and full-order approaches", *J. Wind Eng. Ind. Aerod.*, **90**(12), 1981-1993.

Ge, Y.J. and Xiang, H. (2002), "Statistical study for mean wind velocity in Shanghai area", *J. Wind Eng. Ind. Aerod.*, **90**(12), 1585-1599.

Ge, Y.J. and Tanaka, H. (2000), "Aerodynamic flutter analysis of cable-supported bridges by multi-mode and full-mode approaches", *J. Wind Eng. Ind. Aerod.*, **86**(2), 123-153.

Ge, Y.J., Xiang, H.F. and Tanaka, H. (2000), "Application of a reliability analysis model to bridge flutter under extreme winds", *J. Wind Eng. Ind. Aerod.*, **86**(2), 155-167.

Han, Y., Liu, S.Q. and Cai, C S. (2015), "Flutter stability of a long-span suspension bridge during erection", *Wind Struct.*, **21**(1), 41-61.

Hua, X.G., Chen, Z.Q. and Ni, Y.Q. (2007), "Flutter analysis of long-span bridges using ANSYS", *Wind Struct.*, **10**(1), 61-82.

Hua, X.G. and Chen, Z.Q. (2008), "Full-order and multimode flutter analysis using ANSYS", *Finite Elem. Anal. Des.*, **44**(9), 537-551.

Mayne, J.R. (1979), "The estimation of extreme winds", *J. Wind Eng. Ind. Aerod.* , **5**(1-2), 109-137.

Ostenfeld-Rosenthal, P., Madsen, H.O. and Larsen, A. (1992). "Probabilistic flutter criteria for long span bridges", *J. Wind Eng. Ind. Aerod.*, **42**(1), 1265-1276.

Palutikof, J.P., Brabson, B.B., Lister, D.H. and Adcock, S.T. (1999), "A review of methods to calculate extreme wind speeds", *Meteorol. Appl.*, **6**(2), 119-132.

Pourzeynali, S. and Datta, T.K. (2002), "Reliability analysis of suspension bridges against flutter", *J. Sound Vib.*, **254**(1), 143-162.

Sarkar, P.P., Caracoglia, L. and Haan, F.L. (2007), "Parametric study of flutter derivatives of bluff cross sections and their implications on the aeroelastic stability of flexible bridges", *The 39th technical panel meeting on wind and seismic effects*, US–Japan cooperative program in natural resources (UJNR), Technical Memorandum of PWRI (Public Works Research Institute) No. **4075** (ISSN 0386- 5878), 432-441.

Sarkar, P.P., Caracoglia, L., Jr, F.L.H., Sato, H. and Murakoshi, J. (2009), "Comparative and sensitivity study of flutter derivatives of selected bridge deck sections, Part 1: Analysis of inter-laboratory experimental data", *Eng. Struct.*, **31**(1), 158-169.

Scanlan, R.H. (1997), "Amplitude and turbulence effects on bridge flutter derivatives", *J. Struct. Eng*., **123**(2), 232-236.

Scanlan, R.H. (1978), "The action of flexible bridges under wind, I: flutter theory", *J. Sound Vib.*, **60**(2), 187-199.

CC